Fernández-Ruiz, M. R., Martins, H. F., Costa, L., Martín-López, S. & González-Herráez, M. 2018, "Statistical analysis of SNR in chirped-pulse ΦOTDR", in 26th International Conference on Optical Fiber Sensors, OSA Technical Digest (Optical Society of America, 2018), paper WF16

Available at http://dx.doi.org/10.1364/OFS.2018.WF16

(Article begins on next page)

Statistical Analysis of SNR in Chirped-pulse ΦOTDR

María R. Fernández-Ruiz*, Hugo F. Martins, Luis Costa, Sonia Martin-Lopez, and Miguel Gonzalez-Herraez

Departamento de Electrónica, Universidad de Alcalá, Edificio Politécnico, 28805, Alcalá de Henares, Spain

** rosario.fernandezr@uah.es*

Abstract: The statistical properties of SNR are analyzed for chirped-pulse (CP-)ΦOTDR and compared with traditional ΦOTDR using coherent-detection. CP-ΦOTDR is showed to have drastically narrower (lower variance) SNR distribution, thus providing higher reliability measurements.

OCIS codes: (280.4788) Optical sensing and sensors; (290.5870) Scattering, Rayleigh; (050.1590) Chirping

1. Introduction

Distributed fiber-optic sensors based on phase-sensitive (Φ)OTDR are gaining much attention thanks to their interesting performance in comparison with other distributed sensing technologies (i.e., based on Brillouin or Raman scattering). Their leading advantage relies on their potential for single-shot measurements, which allows performing sensing at acoustic frequencies [1,2]. In spite of their appealing features, ΦOTDR presents several shortcomings that restrain their use for certain applications. One of the most critical issues is the fact that the resulting power trace is a random interferometric pattern with a statistical distribution of intensity along the fiber. As such, there is a nonlinear relationship between the power trace variation and the perturbation suffered by the fiber (which typically manifests as refractive index variations). For this reason, ΦOTDR was initially proposed as a simple vibration sensor, as it was able to detect perturbations but not to quantify them [1].

A solution for the nonlinearity problem in ΦOTDR is to use the phase of the optical trace, which does vary proportionally with the applied perturbation. Hence, if the trace phase is detected, e.g., using coherent detection methods, the perturbation suffered by the fiber can be quantified, enabling the use of ΦOTDR as a temperature or strain sensor [3]. However, the use of coherent detection in ΦOTDR entails additional difficulties. First, the optical trace and the local oscillator must be coherent along the whole fiber length, either imposing the need for extremely high coherent lasers (coherence lengths of twice the fiber size) or reducing the length range of the sensor. A complete phase characterization requires polarization diversity, complicating the detection procedure [4]. But most challenging, phase detection critically depends on the optical signal-to-noise ratio (SNR) of the measured points. Therefore, it is severely affected by the fading points of its interferometric pattern, as well as by phase and amplitude noise in the trace, which may lead to very noisy measurement locations as well as faulty phase unwrapping. The statistical properties of the SNR of phase-measuring ΦOTDR sensors have been recently evaluated, concluding that the sensitivity of these sensors (defined as the minimum input signal required to reach a specified SNR) can vary several decades (>50 dB) from one point to another in the trace [5]. Such an extreme variability severely limits the reliability of ΦOTDR sensors based on coherent detection.

A novel method for interrogating ΦOTDR has been recently proposed with encouraging results. This method is known as chirped-pulse (CP-)ΦOTDR and relies on the propagation of a linearly chirped probe pulse instead of a transform-limited one, as in the traditional case [6]. It has been proved that the linear chirp induces a frequency-to-time mapping that converts the refractive index variations in the fiber to local temporal shifts in the power trace. These temporal shifts are obtained by means of trace-to-trace local correlations, enabling quantification of the perturbations by simply direct detection of the optical trace. Besides, phase noise in the trace due to e.g. the limited coherence of the probe laser, can be measured and mitigated, allowing for high SNR measurements with relatively moderate coherence probe lasers [7].

In this work, we present an analysis of the statistical properties of the SNR and sensitivity of CP-ΦOTDR. We show that the nature of the employed interrogation method permits perturbation quantification almost independently of the trace fading points, an SNR with significant lower variability (~10 dB) and only dependent on the trace optical noise (mainly amplitude noise, as the phase noise is mostly compensated [7]). Hence, we prove that CP-ΦOTDR offers not only a simpler interrogation procedure but also notably higher reliability in the obtained sensing measurements.

2. Statistical properties of chirped-pulse ΦOTDR

In CP-ΦOTDR, the perturbation measurement is performed on the power trace obtained by direct detection. The magnitude optical trace $A(k,t)$ has a Rayleigh distribution, so the detected power trace $A^2(k,t)$ has an exponential distribution (k being the trace index and t the temporal index along the same trace). As introduced in the previous Section, a perturbation Δn in the refractive index, n, of the fiber translates into a local time shift $\Delta t = -\upsilon_0 \cdot (\Delta n/n) \cdot (\tau_p/\delta\upsilon)$ in the power trace, where υ_0 is the central frequency of the probe pulse and $\delta\upsilon$

is the spectral content of the probe pulse chirp [6]. This temporal shift is measured via trace-to-trace local correlations along a time window set by the spatial resolution. In the presence of a perturbation at a position corresponding to $t=l$, the correlation is performed between a signal $x_1(t)=s_1(k,t)+n_1(k,t)$ and $x_2(t)=s_2(k+1,t)+n_2(k+1,t)$, where $s_1(t)=A^2(t)$, $s_2(t)=s_1(t-\Delta t)$ limited by a time window given by $l-\tau_p/2<t<l+\tau_p/2$. The temporal shift is obtained as [8]

$$\begin{aligned}\Delta t &= \arg\max\{x_1(t)*x_2(t)\} \\ &= \arg\max\{R_s*\delta(t-\Delta t)+s_1(t)*n_2(t)+s_2(t)*n_1(t)+n_1(t)*n_2(t)\},\end{aligned} \quad (1)$$

where $*$ refers to correlation, $\arg\max$ stands for the arguments of the maxima, R_s is the autocorrelation of the signal $s_1(t)$, and $n_1(t)$, $n_2(t)$ are considered to be additive Gaussian noise in each signal within the correlation time window (recall that phase noise can be easily compensated in CP-ΦOTDR [7]). Assuming a well-conditioned power trace in terms of SNR, $n_1(t),n_2(t)\ll s_1(t),s_2(t)$, and therefore the term $n_1(t)*n_2(t)$ is negligible with respect to $s_p(t)*n_q(t)$ ($p,q=1,2$). Besides, the noise and signal components are decorrelated, and hence, the second and third terms in the second line of (1) can be considered as noise with equivalent power. In order to obtain the proper value of Δt, it is necessary that the first term in (1) is higher than the second plus third terms. In general, the autocorrelation of a signal with exponential distribution has a peak whose width is inversely proportional to the signal bandwidth and whose energy is proportional to the correlation window. Hence, the condition to measure Δt can be accomplished whenever the signal bandwidth is much higher than the correlation window. This condition ($\delta\upsilon\gg 1/\tau_p$) is systematically satisfied in CP-ΦOTDR, as it is already a condition for its proper operation [6]. Eventually, as long as we can guarantee that the SNR of the detected power trace is high enough, we will be able to measure the signal almost independently of the trace fading points. Note that the trace points with very low power do not impair the perturbation measurement, as we measure the temporal shift of those points with a correlation window much longer than the fading point width.

To perform a statistical analysis, it is important to consider that the acquired trace varies locally at the perturbation position. Hence, an instantaneous perturbation will only affect a region whose width is given by the spatial resolution (imposed by the probe pulse width, τ_p) [6]. For this reason, the followed strategy consists in analyzing different traces at the perturbation position along a sufficiently long time period. Due to environmental and mechanical variations around the fiber, the trace profile at the perturbation location changes in time. Provided that the correlation between (a window of) the trace at the same position at two sufficiently separated times is as low as the correlation between different positions at the same time, this strategy is eventually equivalent to measuring the perturbation in different locations of the same trace.

The statistical distribution of SNR of the acoustic signal (i.e., the signal resulting from the correlations) is finally obtained by calculating the ratio between the perturbation power and the noise variance along the interrogation period. In the following experimental demonstration, we prove that the resulting SNR histograms are much narrower than in the case where phase detection is required and that, under experimental conditions similar to those in Ref. [5], the minimum value of acoustic SNR is always high (>>1).

3. Experimental demonstration and discussion

Figure 1 shows the setup employed for the experimental analysis carried out.

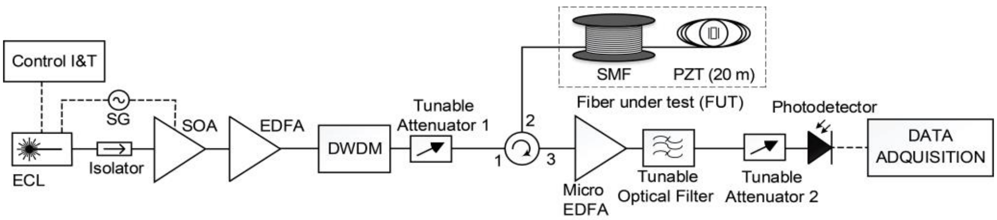

Figure 1: Experimental setup. The acronyms are explained in the body of the manuscript.

First, the chirped probe pulse is generated from an external cavity laser (ECL) whose emitting frequency is set by intensity and temperature (I&T) control, and whose linewidth is 500 kHz. Note that this is at least one order of magnitude higher than linewidths typically reported in ΦOTDR operation with coherent detection (usually of a few kHz). A chirp corresponding to a linear instantaneous frequency with slope 0.01 GHz/ns is induced in the emitted light via linear modulation of the current applied to the laser driver. A super-Gaussian pulse envelope is generated by modulation of the laser output with a semiconductor optical amplifier (SOA). The pulse is then amplified using an erbium-doped fiber amplifier (EDFA) and the amplified spontaneous emission (ASE) is reduced by filtering the signal using a 0.8 nm-bandwidth dense wavelength division multiplexer (DWDM). The chirped pulse is then launched into a sensing fiber of 1 km with a piezo-electric transducer (PZT) at the end. The PZT is employed to induce a controlled perturbation in 20 meters of fiber, in particular, a sinusoidal perturbation with a frequency of 100 Hz and amplitude of 4 V_{pp}, correspondent to a fiber strain of 127 $n\varepsilon_{pp}$. The resulting backscattered trace is amplified by a second stage of EDFA and filter. Finally, the trace is detected using a 1 GHz bandwidth photodetector and acquired at 4 GSps.

As explained in Section 2, the measurement of the perturbation is obtained from correlations applied at the perturbation location along a sufficiently long period of time. This period has to ensure that the trace profile has changed within a window similar to the spatial resolution. It has been verified that under the environmental conditions of our laboratory at the end of the day (i.e., after the central heating is switched off), the trace profile in a temporal window in the order of ~100 ns is uncorrelated with the profile at the same location after a few minutes. This is attributed to both the decrease of temperature plus other mechanical or structural perturbations. Hence, we have performed the analysis along a temporal interval of 6 hours. The procedure explained in the previous section is applied for different probe pulses, namely, with pulse widths of 50 ns, 75 ns and 100 ns, but maintaining the same instantaneous frequency slope (i.e., different chirp-induced bandwidth) and peak power (i.e., different energy). We obtain the acoustic signal, noise and SNR histograms presented in Fig. 2.

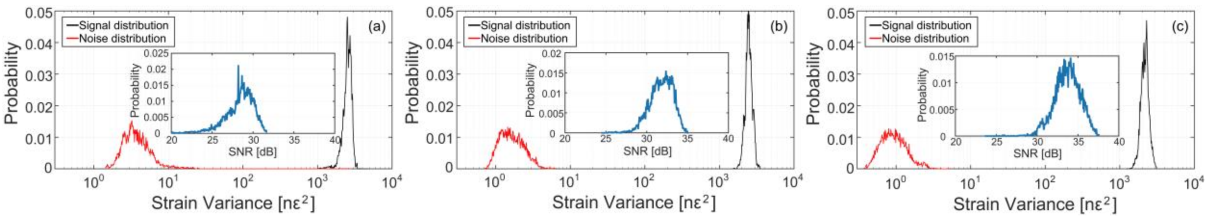

Figure 2: Histograms of acoustic signal, noise and SNR for three different values of probe pulse width: (a) 50 ns; (b) 75 ns and (c) 100 ns. Red line represents the distribution of noise, black line the distribution of the signal, and blue line (insets) the distribution of SNR.

Each plot in Fig. 2 contains two curves plus one inset. Black line represents the histogram of the signal measurement power, while red line represents the histogram of the variances of detected acoustic noise. The signal power has been obtained as the normalized peak of the autopower of the sinusoidal strain signal ($A_\varepsilon^2/2$, with A_ε being the amplitude of the sine). On the other hand, the variance of the noise was obtained as the integral of the normalized power spectral density (PSD) of the acoustic trace along the complete spectral window (RMS value), once the sinusoidal spectral component has been filtered out. The inset shows the calculated SNR, i.e., the ratio between the signal power and the noise variance. The obtained results are summarized in Table 1 and can be interpreted as follows. The signal measurement is independent of the probe pulse width and presents low variance of ~1.5 dB (width at 1/e height), as expected for a linear measurement. The value of variance/width of the histograms in Fig. 2 is provided in dB (ratio between the maximum and minimum values of each curve) due to the high difference in orders of magnitude between the measured signal and noise values. The acoustic noise decreases for higher pulse energies, attributed to the fact that the SNR of the optical trace is also higher for higher values of probe pulse energy. The signal SNR is almost independent of the trace fading points; in 1 km of fiber, the signal is always detected with high (~30 dB) and almost constant (variance of ~4 dB, and width of ~10 dB at 1% at height) level of SNR.

Table 1: Overview of the results depicted in Fig. 2 (values in dB).

	Mean Signal	**Signal Variance**			**Mean Noise**	**Noise Variance**			**Mean SNR**	**SNR Variance**		
Measured at a height of:		*1/e*	*10%*	*1%*		*1/e*	*10%*	*1%*		*1/e*	*10%*	*1%*
50ns	-147	1.4	2.2	3.2	-174	4.2	6.3	11.7	29	4	7	11
75ns	-147	1.6	2.2	3.1	-178	4.8	6.6	8.4	32	4	6	8
100ns	-147	1.4	2.1	3.2	-180	4.8	7.5	8.7	34	4.5	7	9

4. Comparison with SNR distribution in coherent-detection ΦOTDR

Our experimentally obtained results show important differences with those obtained from coherent-detection ΦOTDR. The statistical features of ΦOTDR measurements based on trace coherence detection have been thoroughly analyzed in [5]. There, the authors have determined the expression for the statistical distribution of the SNR and they have provided an experimental analysis that corroborates their analytical results. Recall that in coherent-detection ΦOTDR, the detected phase of the k^{th} trace is $\phi(k,t)=\phi(0,t)+\phi_{signal}(k,t)$, where $\phi(0,t)$ is uniformly distributed in {- π, π }, while $\phi_{signal}(k,t)$ is the phase component providing information about the perturbation. The phase shift accumulates along the fiber length; hence, for a single perturbation a given fiber location, $\phi_{signal}(k,t)$ has a variation proportional to the perturbation from the perturbation location to the end of the fiber. This phase component is obtained by simply subtracting the phase of the reference trace, $k=0$, to all the subsequent traces. To sum up the results obtained in [5], the (acoustic) SNR of detection of an instantaneous perturbation using a sensor based on coherent detection ΦOTDR trace has a random distribution given by:

$$SNR(l,l') = \frac{2\sigma_\phi^2}{\sigma_n^2\left[1/A^2(l) + 1/A^2(l')\right]}, \tag{2}$$

where σ_ϕ^2 is the variance of ϕ_{signal}, σ_n^2 is the variance of the noise, and $A^2(l)$ and $A^2(l')$ are the values of the power trace at a point $t=l$ before the instant corresponding to the perturbation location, and $t=l'$ after the perturbation. Note that $A^2(l)/\sigma_n^2$ is a measure of the optical SNR of the point $t=l$. The authors have obtained the histograms of SNR of the perturbation measurement, calculated from the difference of ϕ_{signal} between arbitrary pair of points l' and l. Under similar experimental conditions (note that identical experimental conditions cannot be applied due to intrinsic differences in the sensing method), the resulting histograms of SNR in the case of coherent detection have a variance several decades wider than in CP-ΦOTDR. In particular, the width at 1/e height of the SNR distribution in their analysis is ~20 dB and at 1% height is 56 dB (more than 4 decades broader than in CP-ΦOTDR). Besides, ~6% of the sensing points are not able to provide a perturbation measurement with enough value of SNR (>1), due to the influence of the exponential distribution of the detected trace (Eq. (2)). The drastically narrower (lower variance) distribution of SNR in CP-ΦOTDR proves the high reliability of chirped-pulse ΦOTDR sensors with respect to the traditional configuration.

5. Conclusions

In this work, we have performed an analysis on the statistical properties of the SNR of sensors based on CP-ΦOTDR and compared the results with a similar study done for traditional ΦOTDR using coherent detection. The two methods are compared under similar conditions (an exact comparison is not possible due to intrinsic differences in the sensing methods) showing clear differences in their statistical properties. While both systems can quantify a perturbation with similar average noise (note that the mean acoustic noise will depend on the optical noise of the trace in both cases), the distribution of the noise is drastically narrower for CP-ΦOTDR. In particular, we have demonstrated that in CP-ΦOTDR, the SNR had a variance of ~4 dB (width at 1/e height) and ~10 dB at a width of 1%, mainly due to the trace additive noise. In contrast, the distribution of SNR in the case of coherent detection presented a variance of ~20 dB (width at 1/e height) and width ~56 dB at 1% height. With such a high variability, a considerable number of trace points are not suitable for sensing. The results can be readily explained by the fact that in coherent detection of traditional ΦOTDR the measurement noise will dramatically increase at points with low optical power. In CP-ΦOTDR however, the temporal shift of points with low power is still accurately measured, so these points do not impair the perturbation measurement. Hence, we have proven that CP-ΦOTDR offers not only a simple interrogation scheme and higher robustness against noise with respect to the traditional ΦOTDR, but also a higher level of reliability in sensing tasks.

6. Acknowledgements and funding

This work was supported in part by: the European Research Council through project U FINE (Grant 307441); the European Commission through project FINESSE MSCA-ITN-ETN-722509; the DOMINO Water JPI project, under the WaterWorks2014 cofounded call by EC Horizon 2020 and Spanish MINECO; the Spanish MINECO through the project TEC2015-71127-C2-2-R; and the regional program SINFOTON-CM: S2013/MIT-2790. The work of LC was supported by EU funding through the project MSCA-ITN-ETN-722509. The work of SML and MRFR was supported by the Spanish MINECO through a "Ramón y Cajal" and "Juan de la Cierva" contracts, respectively.

6. References

[1] A. Barrias, et al., "A review of distributed optical fiber sensors for civil engineering applications," Sensors **16**, 748-782 (2016).
[2] J. Pastor-Graells, et al., "SNR enhancement in high-resolution phase-sensitive OTDR systems using chirped pulse amplification concepts," OL **42,** 1728-1731 (2017).
[3] Z. Wang, et al., "Coherent ΦOTDR based on I/Q demodulation and homodyne detection," OE 24, 853-858 (2016).
[4] M. Ren, et al., "Theoretical and experimental analysis of ΦOTDR based on polarization diversity detection," IEEE PTL 6, 697-700 (2016).
[5] H. Gabai and A. Eyal, "On the sensitivity of distributed acoustic sensing," OL **41,** 5648-5651 (2016).
[6] J. Pastor-Graells, et al., "Single-shot distributed temperature and strain tracking using direct detection phase-sensitive OTDR with chirped pulses," OE **24**, 13121-13133 (2016).
[7] M. R. Fernández-Ruiz, et al., "Laser Phase-Noise Cancellation in Chirped-Pulse Distributed Acoustic Sensors," IEEE JLT **36**, 979-985 (2018).
[8] G. Jacovitti and G. Scarano, "Discrete time techniques for time delay estimation," IEEE TSP **41**, 525-533 (1993).